



Detection and Tracking of Warm Areas on Water Vapour 6.2 μm Satellite Images

J. Novotný*

*Department of Military Geography and Meteorology, University of Defence, Brno,
Czech Republic*

The manuscript was received on 20 May 2008 and was accepted after revision for publication on 18 September 2008.

Abstract:

The paper was focused on verification of relation between potential vorticity anomalies and occurrence of intensive convection via detection of warm areas on satellite WV pictures in the spectral channel of 6.2 μm . In contrast to other papers, however, the dependence was not tested on selected situations but on a common four-month series of data. Within processing three basic methods of detection were checked. The procedure of the most successful option was tracked.

Keywords:

Potential vorticity anomaly, WV satellite imagery, dry intrusion

1. Introduction

In term of cyclonegenesis, knowledge of potential vorticity distribution is a quite useful tool. Although favourable conditions for the existence of convection are often subject first of all to processes of a large scale, the smaller surface formations and effects, which tend to be the initiating mechanism, are usually insufficiently recorded by the model and thus also formable. The convection, which is the result of dynamic processes at high troposphere layers, whether on a synoptic or a mesosynoptic scale, is reflected in a higher degree of the way it is organized and thus also the predictability [1], [2].

Formations, which induce such phenomena, tend to be well-distinguishable in WV pictures. Those are places of tropopause lowering and areas of dry or descending air, which have the appearance of small dark patches, points or belts. These anomalies of tropopause altitude (potential vorticity anomalies) in circulation generally come

* *Corresponding author: Department of Military Geography and Meteorology, University of Defence, Kounicova 65, CZ-612 00 Brno, Czech Republic, phone: +420 973 446 439, fax: +420 973 446 419, E-mail: Josef.Novotny@unob.cz*

from high latitudes and bring dry stratospheric air to lower levels. This indicates that they are an important factor in the development of dynamically induced convection. At these places the stratospheric air with low q_w , which moves over above the low-laid layer of warm air with high q_w , generates the area of potential instability at middle levels [3], [4]. In pictures it actually appears as horizontally not too extensive dark patches and points or belts. The problem is the fact that with dropping of temperature differences at high latitudes such phenomena are hard to observe until they arrive at middle latitudes.

If the "dark eye" advances far to the south, e.g. along circulation of the long-wave trough, the vertical gradient q_w will grow and thus also the probability of development of a large convection will be higher. In case when the formation gets to the area of dynamic ascent, such as on the front side of a long-wave trough (in front of its axis), releasing of the already existing potential instability may occur. The air will ascend along isentropes upwards, i.e. along upwards moving θ surfaces on the front side of anomaly. This ascent will be another contribution to the initiating mechanism of convection just as the configuration of orography and surface effects.

If as one of the basic assumption, the existence of connection between potential vorticity structure, dry intrusions, dry bands, tropopause height and warm dark areas distribution on water vapour images (WV images) is considered, it is possible to set up method of detecting potential vorticity anomalies on searching and tracking areas with higher brightness temperature compared with the surrounding environment.

2. Used Data

For processing data measured by meteorological satellite Meteosat 8 (MSG – Meteosat Second Generation) in the spectral channel $6.2 \mu\text{m}$ (water vapours absorption and emission band) were used. The temporal resolution of sequence was 15 minutes, spatial resolution $3 \times 3 \text{ km}$ at nadir (approximately $4 \times 6 \text{ km}$ in the Central Europe) [5]. Images in original geostationary projection were supplied in the archival format XPIF by the CHMI Satellite Centre.

Period under study covered a time from 1 May 2006 00: UTC till 21 Sept. 2006 23:45 UTC. Approximately 2 % of data were not taken into consideration. To evaluate knowledge on number, location and time of occurrence of detected warm areas data in the graphical format PNG from Czech radar network CZRAD were used. Spatial resolution was $1 \times 1 \text{ km}$ [5], [6]. Time step was 10 minutes. CZRAD data were supplied by the CHMI Radar Section.

With respect to the radar data format, first of all they had to be preprocessed. In order to obtain true radar information, images were trimmed off and then converted by MATLAB Image Tool Processing on two-dimensional matrix. The values characterizing a background and borders were filtered off. Then data were adjusted using georeference and calibration. In next stages of processing, only matrix elements corresponding to radar echo intensity equal or more than 52 dBZ were considered.

3. Principle of Processing

As an initial ideological point was used ISIS method (*Instrument de Suivi dans l'Imagerie satellitaire*) [1] originally developed for detection of cold cloud tops in Meteo France. Subsequently this method was modified by Michel a Bouttier for usage on WV images [8]. Some of criteria and parameters

used were chosen with reference to the results published in the above-mentioned publication.

The procedure can be divided into two steps:

- Detection of warm areas
- Tracking of detected warm areas

3.1. Detection of Warm Areas

The way of detection of warm areas was based on application of spatial determination via temperature criteria. In accordance with an assessment of characteristics for the whole images: minimum temperature T_{\min} , maximum temperature T_{\max} and range of temperature ΔT the values of parameters used in the variants of detection methods were set up.

Three ways of determination (detection) of warm areas divided into eleven variations were tested. Common initial parameter for three detection methods: required minimum temperature T_{\min} , required minimum area S_{\min} and required minimum range of temperature ΔT_d in terms of detected areas. A detailed survey of variants corresponding to parameters is available in [9].

Detection method 1 to determine warm areas is based on application of three basic parameters T_{\min} , S_{\min} and ΔT_d . The variants of this method are simple analogies to horizontal sectional views of spatial distribution of brightness temperature.

In addition to criteria T_{\min} , S_{\min} and ΔT_d , in the **2nd method of detection**, another parameter of required minimum temperature difference between border pixels falling into the detected warm area and neighbouring pixels extrinsic to the detected area ΔT_h (Fig. 1). Temperature difference value was set up $\Delta T_h \geq 0.3^\circ\text{C}$.

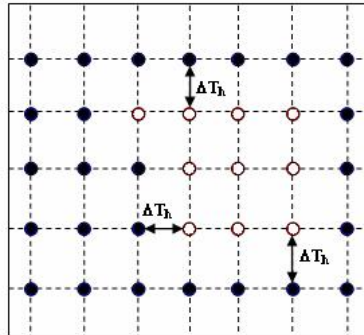


Fig. 1 Scheme of the 2nd method of detection of warm areas (horizontal projection). White points represent pixels falling into the detected area, black points extrinsic to the area. Temperature difference between them $\Delta T_h \approx 0.3^\circ\text{C}$.

The 3rd method of detection is besides three basic parameters based on the criterion of continual decrease or at least constancy of brightness temperature values from pixel with maximal temperature of detected area T_{area}^{\max} towards to the edge of detected warm area (determined by border pixels brightness temperature), then

$T_{\text{area}}^{\text{max}} - T_i \geq \Delta T_d$ (Fig. 2). Temperature values were rounded off by 0.3 °C, 0.6 °C, 1.0 °C for odd variants.

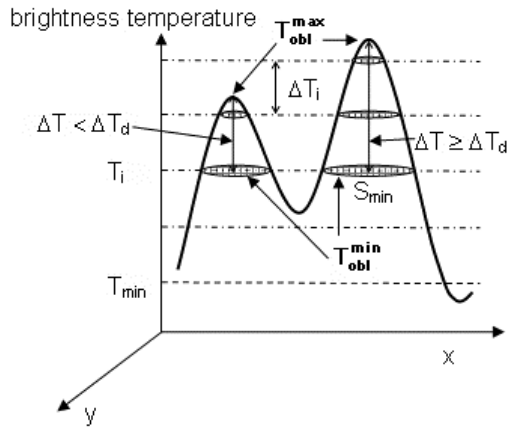


Fig. 2 scheme of the 3th method of detection. T_{\min} is required minimum temperature, T_i is rounded off temperature, ΔT_i represents value of rounding T_i , ΔT difference between $T_{\text{area}}^{\text{max}}$ and T_{area}^{\min} , ΔT_d required minimum range of temperature of detected area, S_{\min} required minimum area. Modified, see [2].

3.2. Comparison of Detected Warm Areas Occurrence and Radar Echoes

In the next phases of processing, data about position and time of occurrence of detected warm areas were compared with occurrence of deep convection (chosen radar echo intensity equal or more than 52 dBZ). During evaluation, the simplified presumption that deep convection clouds develop only in conjunction with presence of upper temperature anomaly was tested (detected warm areas on WV images in this case). Two approaches were used for data processing. In both of them, an occurrence detected areas was searched till time interval up to 24 hours before radar echo registration.

In the 1st approach, presence of detected warm area in the neighbourhood of fixed defined area (determined area within 256 km from both Czech radars) was searched. Warm anomaly was searched in distances: up to 0 km (detected warm area occurred inside defined radar area), 100, 200, 300, and 400 km from the edge of the coverage by Czech radar network. Subsequently, these data were compared with a number of radar echo pixels from cumulative intervals: > 100, > 200, > 300, > 500, > 1000, > 1500 pixels. The terms with lower numbers of pixels were also taken into consideration.

In the 2nd approach a relative position of deep convection cores (pixels with the intensity equal or higher than 52 dBZ) was searched. For each radar echo larger than 9 pixels the centre of gravity was defined. Then searching through the area determined by intervals: 0 to 50 km; 51 to 100 km; 101 to 200 km; 201 to 300 km; 301 to 400 km from centre of gravity was investigated. Results of the 2nd approach were evaluated by an occurrence frequency, the 1st approach by success coefficients POD, FAR, EQS.

3.3. Tracking of Detected Warm Areas

Positions of detected warm areas at the three most successful variants were tracked. In order to designate an area at time t as a predecessor of area at time $t + \Delta t$, the following condition must be satisfied:

$$P(C, C') \geq \min[S(C) \cap S(C')] = 1 \text{ pixel}$$

where:

P is intersection of areas C and C'

C is a detected area on WV image in time t and $S(C)$ is a surface of area C ,

C' is a detected area on WV image in time $t + \Delta t$ and $S(C')$ is a surface of area C' .

Succession is considered provided that:

- Areas C at time t and C' at time $t + \Delta t$ only overlap at least at one pixel.
- Areas C at time t overlaps more than one area at time $t + \Delta t$ at least at one pixel. As the primary successor C' is considered the largest area in the generation, the others are the secondary successors.
- Area C' at time $t + \Delta t$ overlaps more than one area C at time t at least at one pixel, the primary predecessor C is considered the area with the longest history (if more than one predecessor has coeval history, the largest area in the generation is taken into consideration), the others are the secondary predecessors.

By application of these rules, it is possible to define the following events:

- The beginning of trajectory: detected area at time $t + \Delta t$ has not a predecessor at time t ,
- The end of trajectory: detected area at time t has not a successor at time $t + \Delta t$,
- Split of trajectories: detected area at time $t + \Delta t$ has more than one predecessor at time t ,
- Merge of trajectories: detected area at time t has more than one successor at time $t + \Delta t$,
- A complex case: at the same time, splitting and merging between the same areas appeared.

Information concerning the position of detected areas is referred to pixel with the highest brightness temperature $T_{\text{area}}^{\text{max}}$.

The sequence of images is not complete, in order to deal with missing terms, we followed these rules:

- If $\Delta t < 1$ hour, trajectories goes on
- If $\Delta t > 1$ hour, all trajectories end in the last image and start in first next image at time $t + \Delta t$.

4. Processing Results

On evaluating individual methods for area detection, the following characteristics were investigated: number of areas detected, size of areas detected, minimum and maximum temperature, range of temperatures.

4.1. Processing of Temperature Characteristics Results from the Whole Images

Total distribution of all brightness temperature values complied well with normal distribution. Maximum frequency was observed at about 231 K. Values T_{min} were

chosen based on the data evaluated. The following cumulative frequencies of occurrence corresponded to chosen values:

| | |
|-------------------|------|
| 225.15 K (−48 °C) | 8 % |
| 230.15 K (−43 °C) | 40 % |
| 231.15 K (−42 °C) | 48 % |
| 235.15 K (−38 °C) | 78 % |
| 238.15 K (−35 °C) | 91 % |
| 240.15 K (−33 °C) | 96 % |

The set of T_{\min} tested values included also values relatively often exceeded. The reason was to avoid situation when chosen threshold values T_{\min} corresponded to very high temperature quantiles and application of other, rather strict criteria (detection method 2 and 3) would result in deleting a great amount of zones.

4.2. Processing Results if Detected Area Temperature and Surface Characteristics

Data on values of temperature range within detected areas showed to be very interesting. In principle, these data illustrate how and what method and variant detects "deep" area. The greatest temperature range was recorded by detection method 1 and 2. The lowest temperature range was noticed by detection method 3. There was a difference between individual months for temperature characteristics from the whole images as well as for processing within areas detected.

From the results ensue that structure of both the whole images and detected warm areas is not homogeneously even, but a relatively broken one. However, detection method 3 consisting in smoothing by means of temperature value rounding off in order to eliminate an impact of small fluctuations in the field of temperature did not prove itself as being suitable. Rounding off of higher values using this method brings about a relatively rapid increase of number of detected pixels per image. Thus, it can be assumed that at certain value of rounding off, the resulting value of surface of detected area S_{area} would approach to detection method 1. That is why, at other processing, attention was directed especially to detection method 1 and 2.

4.3. Comparison of Occurrence of Detected Areas with Radar Echoes

For higher numbers of radar pixels, warm areas were detected through variants t235c15_gr0 and t235c15_g03 in more than 90 % of cases. From the viewpoint of EQS, the best is the modification of variant out_t240c15_gr0, especially for greater number of considered radar pixels and then variant t235c15_gr03, regardless of modification (determination method). EQS value at variant t235c15_gr0 was negatively influenced by a great number of FAR, especially for modification out. The results reaffirmed insufficient sensitivity of variant rx of detection method 3. The denotation of used methods and corresponding variants together with parameters are shown in table 1 at the end of the paper.

Frequency of detection of warm areas through variants $t235_gr0$, $t240_gr0$ and $t235_gr03$ on occurrence of radar echo cells with intensity higher than 52 dBZ is depicted in Fig. 3.

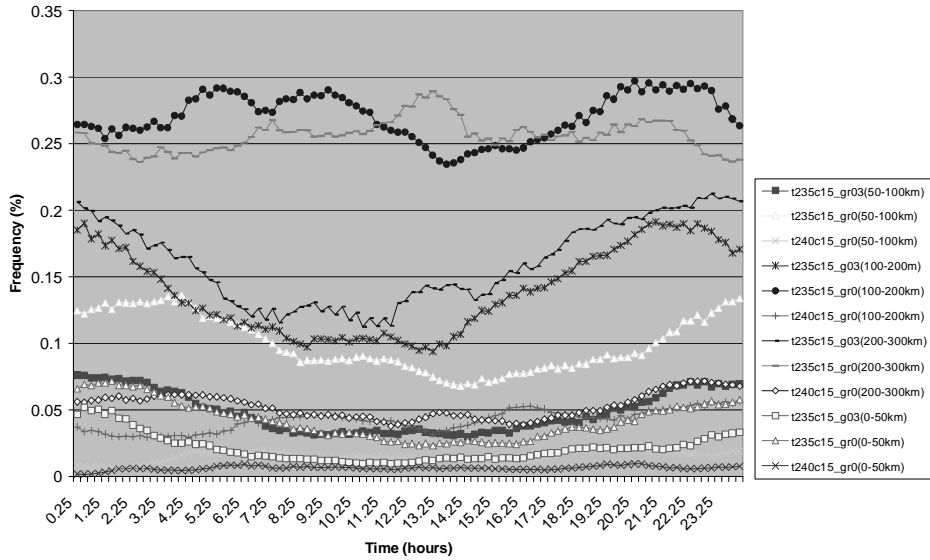


Fig. 3 Frequency of warm areas detection through variants $t235_gr0$, $t240_gr0$ and $t235_gr03$ at occurrence of radar echo cells with intensity higher than 52 dBZ.

The results showed that most commonly (in 25 to 30 % cases), positions T_{area}^{max} of detected areas were located in the distance of $100 \div 200$ km from radar echoes. In terms of time, warm areas occurred most commonly approximately $5 \div 10$ hours before the first registration of intensive convection. The same variant for an interval of $200 \div 300$ km had little lower frequency. Certain delay of increase of frequency in time shown in the Fig. 3 manifests, in fact, an advance of a developed convective cloudiness.

Frequencies of occurrence of detected warm areas through variant $t240c15gr0$ for all distance intervals were relatively low, and in a greater part, there were not more than 5 %. It can be explained that only a small amount of these warm (i.e. deep) temperature (tropopause height) anomalies gets near to the Czech Republic territory. Other maximum frequencies in 20 hour period of time and above was not apparently connected with the influence of detected warm areas, but it was probably caused by a convection in an instable air after passage of a cold front.

However, it should be noted that the disadvantage of the method selected is the fact that a mutual position and direction of movement of detected warm areas and radar echoes was not taken into consideration. A high percentage of FAR was probably due to the fact that into a number of detected areas included were also latent dry bands, which are characterized by only weak or no descending motions, and therefore they do not induce more intensive PV anomalies and i.e. convection. No doubt that results were also influence by a selection of relatively high values of reflective capability (52 dBZ), which corresponds only to very intensive convection. If

the values were lower, the results would be probably more favourable. The disadvantage of the method chosen was the fact that mutual position of detected warm areas and radar echoes was not taken into consideration.

4.4. Evaluation of Geographic Occurrence Of Detected Areas

For an evaluation of geographic occurrence, one variant from detection method 2 and 3 and both variants of detection method 1 was chosen to illustrate a frequency distribution.

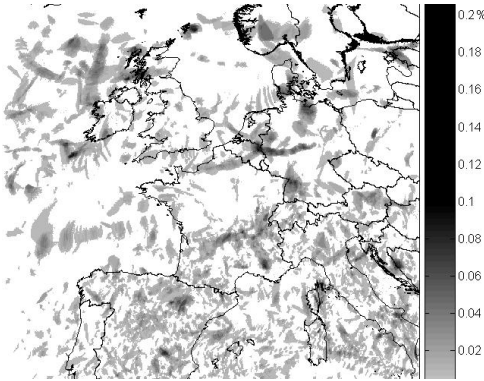


Fig. 4 Frequency distribution of occurrence of detected pixels using a variant rx_235c15_10 for the whole period under

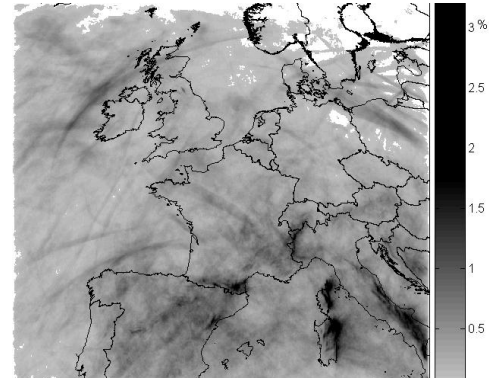


Fig. 5 Frequency distribution of occurrence of detected pixels using a variant t235_gr03 for the whole period under study.



Fig. 6 Frequency distribution of occurrence of detected pixels using a variant t235c15_gr0 for the whole period under study.

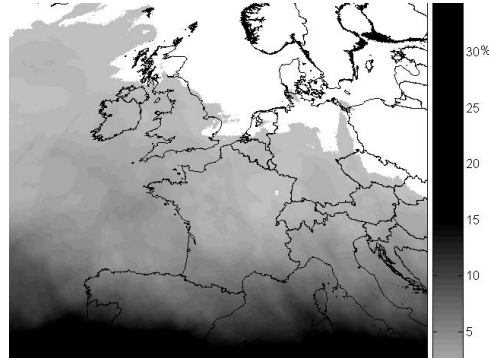


Fig. 7 Frequency distribution of occurrence of detected pixels using a variant t240c15gr0 for the whole period under study.

Visualized results of variant rx_235c15_10 of the detection method 3 (Fig. 4) reveal in principle uniform frequency distribution occurrence within geographic region under study. Even though clusters do not directly indicate a character of paths of detected warm areas or dry intrusions, from the figure it is evident that occurrence of

areas detected by this variant in the North was concentrated into a smaller number of areas compared with the South. Using detection method 2, which was represented by variant t235_gr03, the maximum number of detected pixels was higher in order compared with method 3, even though also here, a frequency of distribution of pixels on the greater part of studied area was not more than 1 % (Fig. 5). Results for variant t235c15_gr0 and t240c15_gr0 detection method 1 confirmed a zone character of distribution of detected pixels (Fig. 6, Fig. 7).

Results show that very deep, and thus intensive intrusions occur more in the West than in the East and rather above the sea than above the land. From this can be drawn a partial conclusion that probability that moving cold front will be accompanied by a dry intrusion, which can cause instability of a part of troposphere and accordingly possible generation of intensive convection, is higher above Western Europe than above Central Europe. A low percentage of occurrences especially for variant of method 3 prove a low detection capability. Based on the results, all rx variants were excluded from further processing.

4.5. Evaluation of Tracking Of Detected Warm Areas

Evaluation of tracking focused on three variants that were the most successful in terms of detection: t235c15_gr03, t235c15_gr0 and t240c15_gr0.

The number of registered trajectories decreased exponentially with an increase of the length (Fig. 8).

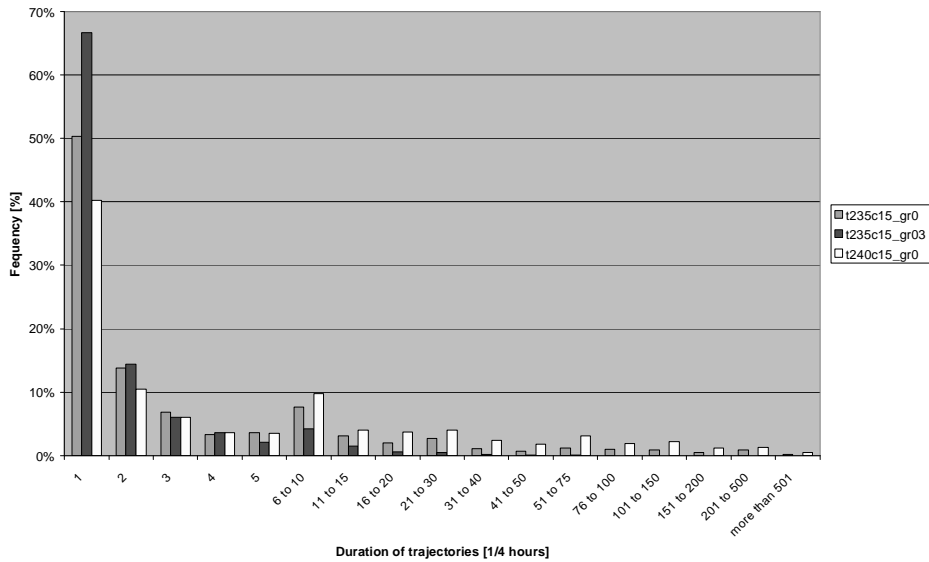


Fig. 8 Frequency of occurrence of registered trajectories for variants t235c15_gr03, t235c15_gr0 and t240c15_gr0.

In accordance with the expectation, warm areas detected only in one period showed the greatest frequency of occurrence. Frequency of occurrence of these cases from the total number of registered trajectories of these cases was at all three considered variants at least 40 %.

Approximately 15 % of all registered trajectories lasted 2 periods, i.e. 0.5 hour. Shorter trajectories prevailed at variants t235c15_gr03 and t235c15_gr0. With a time of duration more than one hour, higher frequency of trajectories showed variant t240c15_gr0. It could also be due to an interruption of trajectories because of the data dropout.

An assessment of direction of movement of detected warm areas for considered variants shows that for all areas, a component of motion from the West (Fig. 9 a, b, c) prevailed. Only a negligible number of trajectories showed an Eastern component of motion. But it is rather attributable to changes of position of the selected reference point, which determined a position of the detected area, i.e. $T_{\text{area}}^{\text{max}}$ point. Figure also indicates that Western component of motion increased with the length of trajectory of detected warm areas.

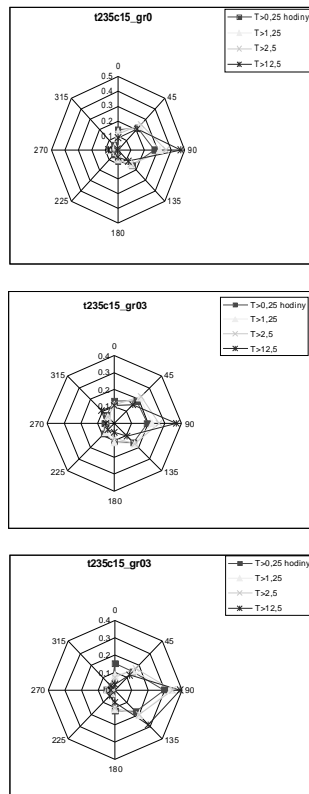


Fig. 9 Frequency of directions of movement of detected warm areas for variants (a) t235c15_gr03, (b) t235c15_gr0 and (c) t240c15_gr0

Coincidence in direction of movement of warm areas detected by the above mentioned variants corresponds to theoretical assumptions on direction of movement of potential vorticity anomalies (anomalies of the tropopause height). It can be assumed that proposed variants of detection really register dry intrusion. However, a more precise estimate of the occurrence would be a speculation since in the numbers passive latent dry zones are included. This probably explains the fact that not always

prior a development of intensive convection as show the results of tests of success coefficients preceded an occurrence of warm area detected by any of three considered variant for detection of detected warm area.

5. Conclusion

The aim of chosen detection method and tracking of warm areas was to verify a validity of dependence of developed convective cloudiness just on the occurrence of the above-mentioned warm areas for the Central Europe region. Data analysis provided a rather divided structure of the whole images, including detected warm areas. However, solution using the detection method 3 consisting in smoothing out by means of rounding off temperature values, which was to eliminate an influence of small fluctuations in the field of temperature, did not prove itself. This is the reason why attention was focused especially on detection method 1 and 2.

Every detection method should be tested to adjust its parameters or to amend other criteria. Cases of detection of areas not evidently connected with the anomalies of potential vorticity are a weak point of every detection variants. This issue can be solved either by filtering off based on geographic determination or by connecting a detection of warm areas to rear side of the cold fronts or jet streams. This could increase a probability that only dry intrusions or dry dynamic bands, which are also connected with the occurrence of PV anomalies, will be detected. With respect to the westward component of motion, it is also possible to filter off false dry intrusions in the South using a condition, which would take into account only those detected warm areas, which have northward or westward component of motion.

Tab. 1 Used method, variants and corresponding parameters

| | 1 st .method | | 2 nd method | | | | 3 rd method | | | | |
|----------------------|-------------------------|-------------|------------------------|--------------|--------------|--------------|------------------------|--------------|--------------|--------------|-------------------|
| | t235c15_gr0 | t240c15_gr0 | t225c15gr_03 | t230c15gr_03 | t235c15_gr03 | t238c15_gr03 | rx_231c15_03 | rx_235c15_03 | rx_235c15_06 | rx_235c15_10 | rx_235c15_03_h1c5 |
| T_{\min} [°C] | -38 | -33 | -48 | -43 | -38 | -35 | -42 | -38 | -38 | -38 | -38 |
| Rounding of T [°C] | | | | | | | 0.3 | 0.3 | 0.6 | 1.0 | 0.3 |
| ΔT_d [°C] | 2.2 | 2.2 | 2.2 | 2.2 | 2.2 | 2.2 | 2.2 | 2.2 | 2.2 | 2.2 | 1.5 |
| T_h [°C] | 0 | 0 | 0.3 | 0.3 | 0.3 | 0.3 | | | | | |

Regarding its practical use, the proposed algorithm of the detection method 1 is implemented in the diagnostic-analytical application VISUAL WEATHER developed for operative utilization in the facilities of the Defence University Military Geography

and Meteorology Department. Discussed is also its use by the Prague Hydrometeorological Support Division of the Military Geographical and Hydrometeorological Office. Because of the results achieved, application of detection methods 2 and 3 in operation is not momentarily taken into consideration.

References and other Sources of Information

- [1] HOSKINS, B. J. A potential vorticity view of synoptic development, *Meteor. Appl.*, 1997, 4, pp. 325-334.
- [2] SANTURETTE P. and GEORGIEV C. G. *Weather analysis and forecasting: Applying satellite water vapor imagery and potential vorticity analysis*, Elsevier Academic Press, 2005, 179 p.
- [3] FRITZ, S. and LASZLO I. Detection of water vapour in the stratosphere over very high clouds in the tropics, *J. of Geophysical Research*, 1993, 98, pp. 22959-22967.
- [4] MANSFIELD, D. The use of potential vorticity as an operational forecast tool. *Meteor. Appl.*, 1996, 3, pp. 195-210.
- [5] ŘEZÁČOVÁ, D., KAŠPAR, M., NOVÁK, P., SETVÁK, M. *Physics of clouds and precipitation* (in Czech), Prague : Academia, 2007, 576 p.
- [6] <http://www.chmi.cz/meteo/sat/>
- [7] MOREL, C. and SENESI, S. A climatology of mesoscale convective systems over Europe using satellite infrared imagery. I. Methodology, *Q. J. R. Meteorolog. Society*, 2002, 128, pp. 1953-1971
- [8] BOUTTIER, F. and MICHEL, Y. Automated tracking of dry intrusions on satellite water vapour imagery and model output, *Q. J. R. Meteorolog. Society*, 2006, 132, pp. 2257-2276.
- [9] NOVOTNÝ, J. *Application of new methods and knowledge of dynamic meteorology into operating practice* (in Czech) [PhD Thesis]. Brno: University of Defence, 2008, 123 p.